

## Characterization of carbonated serpentine using XPS and TEM

Roland K. Schulze, Mary Ann Hill <sup>\*</sup>, Robert D. Field, Pallas A. Papin,  
Robert J. Hanrahan, Darrin D. Byler

*Materials Science and Technology Division, Los Alamos National Laboratory, Los Alamos, NM 87545, USA*

Received 17 November 2003; accepted 4 February 2004

Available online 18 March 2004

---

### Abstract

With the increasing concentration volume of carbon dioxide in the atmosphere, there has been an increasing interest in carbon dioxide sequestration. One method is to store the carbon dioxide in mineral form, reacting solution dissolved CO<sub>2</sub> to precipitate carbonates. In order to understand whether or not such an endeavor is feasible, the carbonation reaction must first be understood. In this study, the surface of ground serpentine, untreated, heat treated and following a carbonation experiment, has been characterized using X-ray photoelectron spectroscopy (XPS) and transmission electron microscopy (TEM). The results indicate that the mechanism for the reaction involves dissolution of the serpentine through the formation of an amorphous phase and subsequent precipitation of magnesite. The rate limiting step appears to be the diffusion of Mg out of the amorphous phase.

© 2004 Elsevier Ltd. All rights reserved.

*Keywords:* X-ray photoelectron spectroscopy; Serpentine; Lizardite; Carbonation; CO<sub>2</sub> sequestration; Transmission electron microscopy

---

### 1. Introduction

There is increasing interest in studying the disposal of carbon dioxide, one of the primary greenhouse gases linked to global warming. The successful disposal of carbon dioxide could have a great impact on global warming. One method currently being investigated is chemical fixation of carbon dioxide in the form of carbonate minerals [1,2]. The process involves a solution of sodium

---

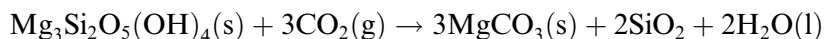
<sup>\*</sup> Corresponding author. Fax: +1-505-667-2264.

E-mail address: [mahill@lanl.gov](mailto:mahill@lanl.gov) (M.A. Hill).

bicarbonate ( $\text{NaHCO}_3$ ), sodium chloride ( $\text{NaCl}$ ) and water mixed with serpentine mineral powder ( $\text{Mg}_3\text{Si}_2\text{O}_5(\text{OH})_4$ ). Carbon dioxide is then dissolved into the slurry at an elevated temperature and pressure to enhance the kinetics of the reaction. The result is conversion of the carbon dioxide to a thermodynamically stable form, magnesite ( $\text{MgCO}_3$ ). Seifritz first proposed this as a natural means of storing  $\text{CO}_2$  generated from the burning of fossil fuels [3]. With this method, environmentally benign and thermodynamically stable waste products are created. There is no risk of releasing  $\text{CO}_2$  into the atmosphere at the disposal site as it is chemically bound in a natural mineral form.

Calcium and magnesium oxides are the only common oxides that readily form carbonates. Magnesium bearing deposits are frequently richer than deposits containing calcium oxide. Thus, magnesium bearing minerals are more attractive for  $\text{CO}_2$  sequestration. The mineral chosen for this study is serpentine, with a structure consisting of alternating silicate tetrahedral sheets and brucite octahedral sheets. The three polymorphs of serpentine are antigorite, lizardite and chrysotile. The structure of antigorite is corrugated; lizardite consists of topological layer; and chrysotile is cylindrical [4]. This mineral, in the purest form, contains 43 wt.%  $\text{MgO}$ , the starting material for the carbonation process.

The carbonation of serpentine in natural deposits occurs slowly. To develop an economically feasible carbon sequestration process, the reaction kinetics must be accelerated. This has been achieved by using elevated temperatures and pressures, adding sodium chloride and sodium bicarbonate to the aqueous solution, grinding the serpentine to increase the surface area and heat treating the serpentine prior to the carbonation reaction to cause dehydroxylation and thereby increase the magnesium oxide content by weight in the starting material. Studies indicate that heat treated (dehydroxylated) samples carbonate more readily than untreated samples [5]. A dramatic increase in carbonation reactivity is associated with samples heat treated at 630 °C, with higher temperatures providing little increase in reactivity [6]. The carbonation process begins when carbon dioxide is dissolved in water to form carbonic acid ( $\text{H}_2\text{CO}_3$ ). The carbonic acid dissociates into  $\text{H}^+$  and  $\text{HCO}_3^-$ . The  $\text{H}^+$  ions are then exchanged with  $\text{Mg}^{2+}$  cations on the mineral surface forming silicic acid ( $\text{H}_2\text{O}_3\text{Si}$ ) or silica ( $\text{SiO}_2$ ) and water. The free  $\text{Mg}^{2+}$  cations then react with bicarbonate ions to form magnesium carbonate ( $\text{MgCO}_3$ ). The proposed carbonation reaction is as follows:



$$\Delta H_{\text{reaction}} = -63.6 \text{ kJ/mol CO}_2 \text{ (exothermic)}$$

O'Connor et al. describes aqueous media mineral carbonation in greater detail [7,8].

In order for the carbonation process to proceed,  $\text{MgO}$  needs to be removed from the serpentine. However, if a mineral dissolves incongruently or nonstoichiometrically, a surface layer can form with a composition different than that of the bulk. Such a layer may inhibit the diffusion of ions across the interface between the mineral surface and the solution. Thus, this layer can be the rate limiting feature in the carbonation process. Luce et al. noted the incongruent dissolution of magnesium silicate [9]. The work of Lin and Clemency [10] supported this research, finding that magnesium from the octahedral sheets in antigorite, talc and phlogopite was more likely to be released than silicon from the tetrahedral sheet. Tartaj et al. [11] observed a lack of  $\text{Mg}$  in particle

surface layers during dissolution experiments, resulting in low isoelectric point values in some serpentine samples.

The purpose of this study is to understand the dissolution of the serpentine as a result of the carbonation process. To accomplish this, it is imperative to characterize the surface of the materials. The current investigation has utilized X-ray photoelectron spectroscopy (XPS) and transmission electron microscopy (TEM) to characterize the surface of the carbonated powders.

## 2. Experimental procedure

Bulk serpentine of the lizardite polymorph was crushed using a jaw crusher set to its smallest opening to produce the finest size fraction of material possible. The crushed material was then ground to a size passing a 200 mesh sieve (157  $\mu\text{m}$ ) in a Spex shatterbox. This process was repeated until sufficient material was produced to complete several experiments. Size fractionation of some of the powder was accomplished using gravity separation. A dispersant of sodium metahexaphosphate ( $\text{NaPO}_3$ )<sub>6</sub> was used during the process. Heat treated samples were placed in a Lindberg thermolyne furnace, evacuated to 300 mTorr, backfilled with  $\text{CO}_2$  gas, and then held at 630 °C for 3 h.

The direct solution carbonation experiments used a Haskel 30-152 H two stage, high pressure gas booster to achieve pressures up to 5000 psi. The following materials were placed in the Parr autoclave system: 69.64 g of serpentine, 850 cc of water (serpentine is hydrophilic), 1 M NaCl (a flux), and 0.64 M  $\text{NaHCO}_3$  (the maximum solubility at room temperature). The vessel was then sealed and purged with  $\text{CO}_2$ . The autoclave was operated at 2300 psi and 155 °C for 2 h. The sample mixture was stirred at 1490 rpm. Three samples were analyzed using XPS: untreated serpentine (as-ground), serpentine heat treated at 630 °C in flowing  $\text{CO}_2$  for 3 h and heat treated and subsequently solution carbonized material with a 22% conversion to carbonate.

A Physical Electronics 5600ci XPS analyzer was used with Al  $K\alpha$  X-rays (1486.6 eV). The binding energies were corrected to the C1s peak at 284.8 eV. Atomic concentrations were calculated using the following relative sensitivity factors: C1s (0.314), O1s (0.733), Na1s (1.102), Mg2s (0.274), Si2p (0.368) and Fe2p (2.946). The serpentine powders were mounted on conductive carbon tape. The sampling depth into the surface of the serpentine particles was approximately 50–70 Å. In addition various monolithic standards ( $\text{MgO}$ ,  $\text{Mg(OH)}_2$ ,  $\text{MgCO}_3$ ) were procured or produced for spectral comparison purposes.

Specimens for TEM examination were prepared from material sieved to the 0.25–5  $\mu\text{m}$  diameter range. Selection of this small size fraction was necessary for electron transparency. The powder was dispersed in isopropyl alcohol using an ultrasonic bath, and samples were floated onto holey carbon Cu grids. These were analyzed in a Phillips CM30 instrument, operating at 300 KeV, equipped with a PGT thin window EDS detector.

## 3. Results

A scanning electron micrograph of the starting serpentine powder is shown in Fig. 1. The particles are irregular in size and shape with relatively smooth edges and surfaces, resulting from

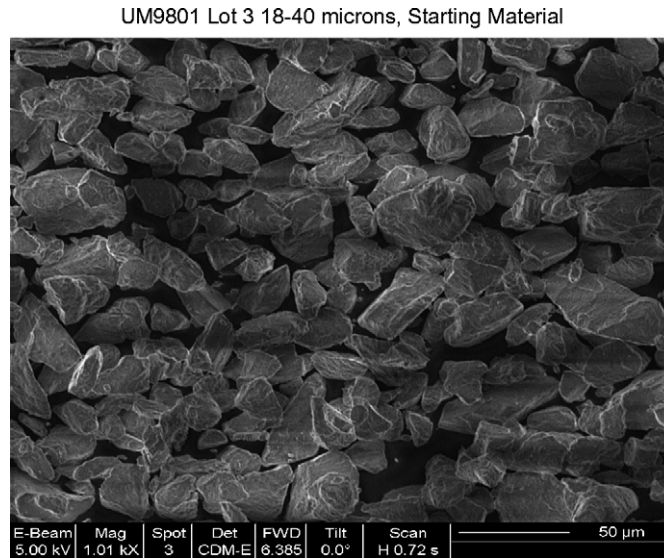


Fig. 1. Scanning electron micrograph of the serpentine starting powder, 18–40  $\mu\text{m}$  size fraction.

fracture during attrition. XPS survey scans of the three materials, shown in Fig. 2, were qualitatively the same, although subtle differences in the relative intensities of the Na, Mg and C peaks

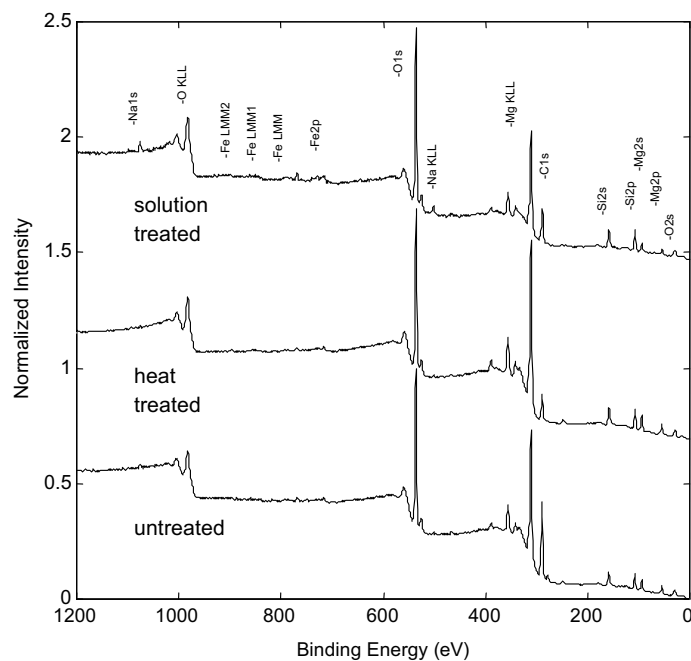


Fig. 2. XPS survey scans of serpentine in the untreated, heat-treated, and solution-treated conditions.

were observed. A close examination shows enhanced Si relative to Mg at the surface of the solution treated sample as compared to the other samples. These results immediately suggest that the autoclave solution treatment preferentially leaches Mg from the surface, leaving a layer rich in Si.

Representative high resolution XPS results for the Si2p peak and the Mg2s peak for the three classes of sample treatment are shown in Fig. 3. The broad peaks suggest that a distribution of chemical states is present. The salient features of this experiment indicate that while the heat treatment causes a slight reduction in the average Si chemical state (shift to lower binding energy) and a slight oxidation in the average Mg chemical state (shift to higher binding energy), the relative amounts of Si and Mg remain the same as in the untreated sample. The binding energy of the Si2p peak for these two samples is approximately 103.0 eV, consistent with silicon in a silicate matrix [12]. Upon CO<sub>2</sub> solution treatment, the surface becomes enriched in Si relative to Mg by almost a factor of two over the untreated material. This silicon rich surface layer may be a passive layer (diffusion barrier) that results in poor reaction conversion in the bulk of the particle. In addition, the Si2p peak shifts to a higher binding energy of 103.5 eV, consistent with the formation of silica (SiO<sub>2</sub>) [12]. The Mg2s binding energy is relatively invariant with chemical state, so chemical changes can be difficult to detect.

Fig. 4 shows a high resolution scan of the O1s XPS peak. The heat treated sample shows a lower O1s binding energy (531.7 eV) than the untreated sample (532.0 eV), consistent with the removal of hydroxyl groups (which appear at higher binding energy in the O1s) at the surface. The solution treated sample shows a higher O1s binding energy (532.5 eV) than the untreated sample

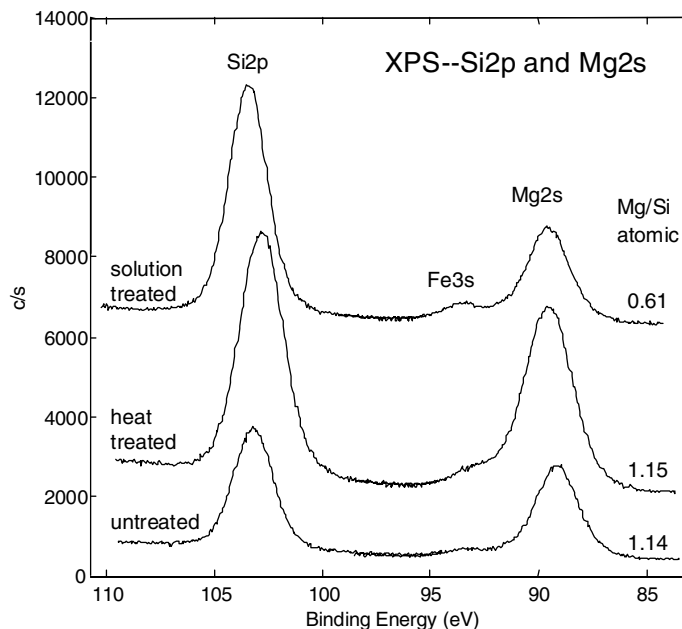


Fig. 3. XPS analysis for various treatments of serpentine. The Si2p and Mg2s peaks are indicated. Note relative intensities of these two peaks. Surface atomic concentration ratios of Mg/Si are also shown for the various treatments.

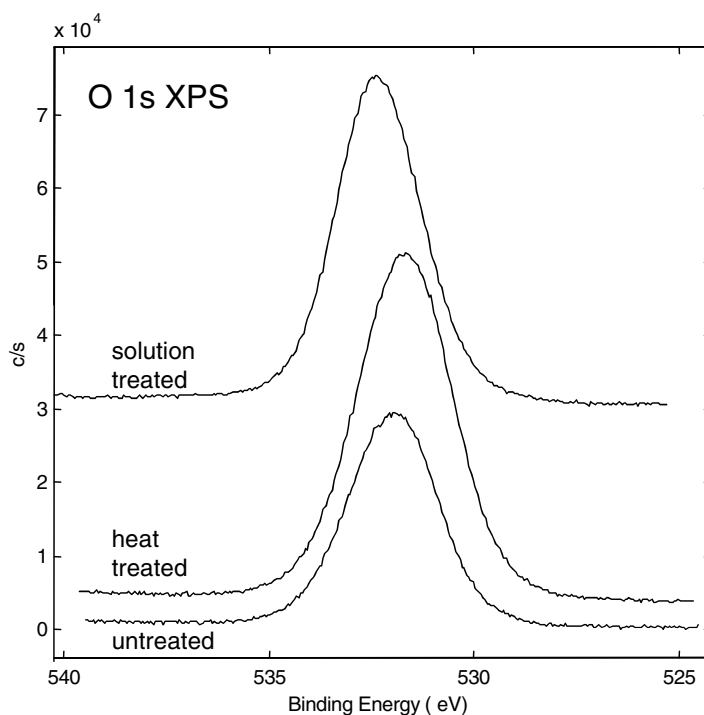


Fig. 4. A high resolution scan of the O1s peak.

(532.0 eV), indicating a possible addition of hydroxyl groups to the silicon rich layer at the surface. Again, the broad peaks are indicative of a range of chemical states present.

A high resolution scan of the C1s XPS peak shows the presence of a high binding energy feature at 290.5 eV that is undoubtedly a carbonate. Although it was difficult to interpret the C1s peaks unambiguously due to the sample handling and exposure of the sample to the atmosphere after reaction (different amounts of adventitious carbon from sample handling), the observed chemical shift of the carbonate feature indicates that this is an ionic metal carbonate, as opposed to an organic carbonate.

Table 1 shows the atomic concentration results from the XPS scan. The carbon concentrations are not necessarily representative of the serpentine samples due to preparation artifacts from the mounting tape or handling prior to analysis. The Na and Fe concentrations increase following solution treatment. The Mg:Si ratio decreases after solution treatment by almost a factor of 2, indicating that the surface is depleted in Mg relative to Si after solution treatment.

Table 1

The atomic concentrations of the surface of serpentine samples using XPS

	C	O	Na	Mg	Si	Fe	Mg/Si
Untreated	46.7	37.7	0.4	7.7	6.8	0.8	1.14
Heat treated	24.2	49.8	0.3	13.2	11.5	1.0	1.15
Solution treated	31.0	47.8	1.5	6.8	11.2	1.5	0.61

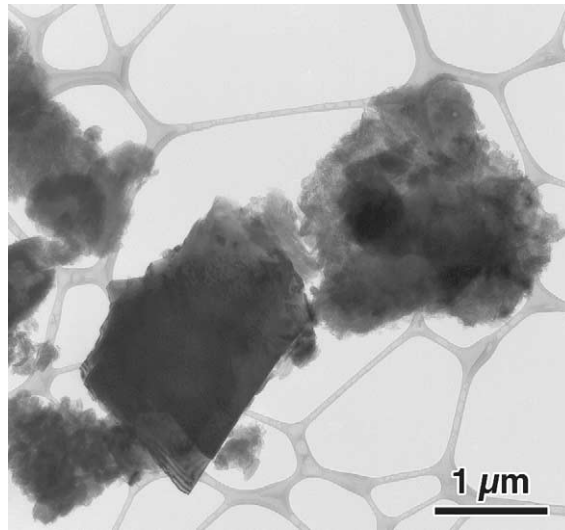


Fig. 5. TEM micrograph of 2.5–5  $\mu\text{m}$  serpentine particles following carbonation experiment. Particles are mounted on a holey carbon grid.

TEM analysis of 0.25–5  $\mu\text{m}$  solution treated serpentine powder revealed three predominant features: magnesite particles, lizardite particles and an amorphous phase. The magnesite and lizardite phases were identified by selected area electron diffraction (SAD). The magnesite particles displayed strong diffraction contrast and were generally highly faceted. The most prominent facets were on the  $\{10\bar{1}4\}$  planes, a well known growth plane for this structure [13]<sup>1</sup>. The lizardite particles displayed weaker diffraction contrast and more diffuse reflections in the diffraction patterns, which tended to deteriorate under the electron beam. These particles were generally surrounded by the amorphous phase, while the magnesite particles were more likely to have surfaces free from the amorphous material. TEM micrographs displaying all three of these features are shown in Figs. 5 and 6. The EDS spectra corresponding to points 1 (magnesite), 2 (amorphous phase) and 3 (lizardite) in Fig. 6 are shown in Fig. 7. The Cu signal is an artifact from the Cu grid on which the particles were deposited. Mg, Si and O are noted in the amorphous phase and the lizardite, while the Si peak is absent in the magnesite. A small Fe peak is associated with all of the phases.

#### 4. Discussion

Luce observed three types of kinetic behavior in studying the dissolution kinetics of magnesium silicates [9]. The first was rapid surface ion exchange corresponding to a layer thinner than one unit cell. It has been proposed by Guthrie et al. [14] that the carbonation process is dominated by dissolution and precipitation as opposed to direct carbonation of the magnesium silicate.

<sup>1</sup> Indices are for the X-ray smallest cell,  $a_{\text{hex}} = 0.463 \text{ nm}$ ,  $c_{\text{hex}} = 1.502 \text{ nm}$ .

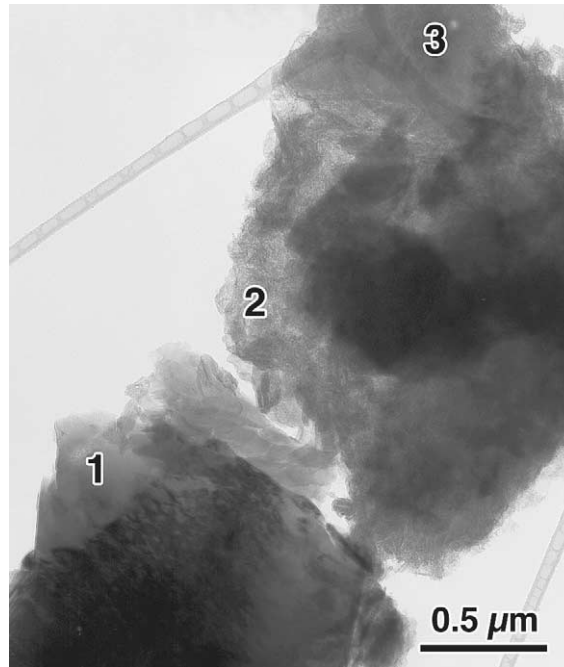


Fig. 6. Higher magnification TEM micrograph of area in Fig. 5, showing magnesite particle in the bottom left corner and lizardite particles surrounded by an amorphous phase in the upper right corner.

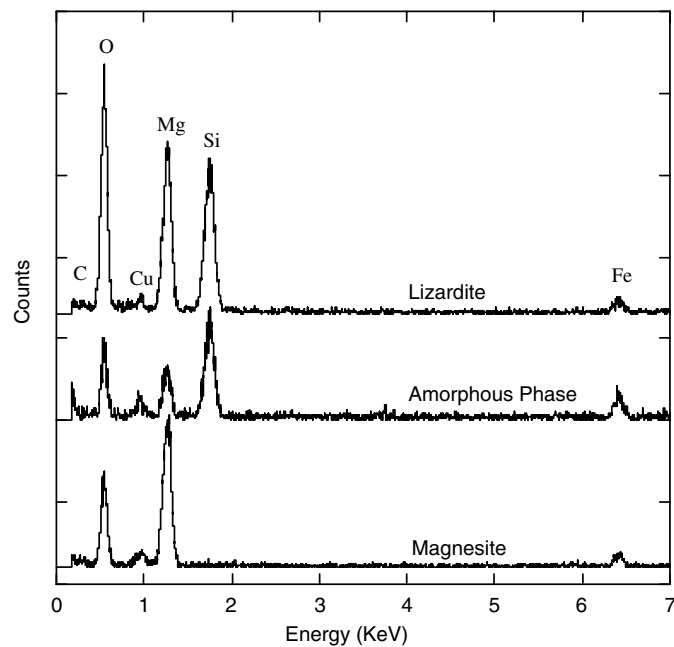


Fig. 7. EDS spectra from areas in Fig. 6 for (1) large crystalline magnesite, (2) amorphous phase, and (3) lizardite.



Although  $\text{Mg}^{2+}$  may be released through rapid cation exchange with  $2\text{H}^+$ , this effect is assumed to be minimal since the silicate structure is unsuitable for rapid cation diffusion at low temperatures. The second type of kinetic behavior is slow linear extraction of cations in strong acid solutions. In the current study, the pH was not measured in situ during the carbonation process, but it is probably dominated by bicarbonate (mid pH) and perhaps carbonic acid (low pH) [14]. Thus, this mechanism is unlikely to be operative. The third type of kinetic behavior is slow parabolic thin film diffusion controlled cation extraction in mild acid to alkaline solutions. Over longer periods, Luce observed parabolic kinetics at all solution pH values except 1.65 [9]. The parabolic kinetics are consistent with diffusional transport limited processes. The instantaneous rate can be affected by mineral grinding as the dissolution rates of deformed surfaces and fine particles will be high initially [15–18]. The dissolution rates then become linear with time, consistent with either surface limited reactions or diffusion controlled reactions across a layer of constant thickness:

$$\text{Rate} = dC/dt = k_p t$$

where  $k_p$  is the reaction rate constant, and  $t$  is time [19].

If congruent dissolution were to occur, a Mg:Si ratio of 1.5 is expected. The Mg:Si ratio for the solution treated sample, shown in Table 1, is 0.6. This is indicative of incongruent dissolution that has been observed for lizardite dissolved under similar conditions by Luce et al. and Guthrie et al. [9,14]. In chemical weathering, kinetic models have found that incongruent dissolution occurs initially with the rapid migration of a specific constituent [20]. In this case, magnesium diffuses rapidly into the aqueous phase leaving behind a layer enriched in silicon. After this initial period of incongruent dissolution, dissolution is expected to proceed congruently.

A significant qualitative result from the TEM studies is the ubiquitous nature of the Mg peak; specifically, the failure to find any amorphous phase with just Si and O and no Mg. Nonetheless, it is clear that the presence of the amorphous silica layer on the surface of the serpentine particles affects the carbonation rate and mechanism. The thickness of the layer ranges from 40 to 100 nm, based on the TEM images. In order for the reaction to proceed, Mg would have to diffuse across the layer of amorphous silica. The transport of cations in silica is so slow that it is usually not measurable at temperatures below 1000 °C. Even in polycrystalline quartz, cation transport occurs principally along defects and grain boundaries rather than through lattice transport. It is apparent that the Mg noted in the amorphous silica layer is trapped and will not diffuse to the surface to be carbonated in a realistic time frame. Therefore, unless the solution chemistry can be modified to dissolve silica (e.g. through addition of  $\text{F}^-$  to the solution), then the reaction will not approach completion for particles of this size in any reasonable time frame.

Two explanations can be suggested for the ubiquitous presence of Mg in the amorphous phase. The first is simply that the reaction does not go to completion, so that the byproduct is a mixed Mg–Si oxide (amorphous silica with Mg in solution), however this simple mechanism does not explain all of the observed microstructure. Therefore, we propose that the initial step in the process is the breakdown of the lizardite crystal structure. The magnesite then grows from this amorphous product, with the rate limiting step being the diffusion of Mg out of the amorphous phase. In this case, the reaction still does not go to completion, as it is limited by the transport of Mg (presumably  $\text{Mg}^{2+}$  cations) through amorphous silica. This latter mechanism is then limited by the formation of a continuous silica layer (with Mg in solution) that acts as a barrier to further diffusion. This would not only explain the absence of pure  $\text{SiO}_2$ , but the frequent observation of

pure magnesite particles with little or no surrounding amorphous phase (i.e. the Mg diffuses out of the amorphous phase, forming magnesite on the edges, rather than the SiO<sub>2</sub> being pushed out of the growing magnesite). De la Caillerie et al. detected an amorphous silicate during contact of solvated Mg<sup>2+</sup> cations with silica and moderately basic pH [21]. A Si–O–Mg bond was found with nuclear magnetic resonance (NMR), showing that the Mg was fixed through the formation of a high surface area, amorphous phase described as a magnesium silicate gel layer on a silica surface. In De la Caillerie's study, there was no evidence of a dissolution–precipitation kinetic effect where the absorption of the magnesium disturbed the chemical environment to such an extent that the Si–O bonds were weakened. These observations are consistent with the proposed mechanism as well as the observations in XPS where, upon solution treatment, the Si chemical form changes from one that is silicate-like to one that is silica-like.

## 5. Conclusions

The carbonation of ground serpentine was studied to determine the feasibility of converting carbon dioxide to a thermodynamically stable form, magnesite (MgCO<sub>3</sub>). Serpentine before and after treatment in a CO<sub>2</sub> reaction vessel was characterized using X-ray photoelectron spectroscopy and transmission electron spectroscopy to provide a better understanding of the surface reactions occurring during the carbonation process. The XPS and TEM data show that a Mg containing silica layer is formed around the serpentine following carbonation. Diffusion of magnesium from this amorphous phase is believed to be the rate limiting step in the carbonation reaction. In order for this process to be used for carbon dioxide disposal, the solution chemistry must be modified to facilitate dissolution of this amorphous silica layer.

## Acknowledgements

We gratefully acknowledge the support of Los Alamos National Laboratory through the laboratory directed research and development program. We thank Hans Ziock and George Guthrie for many useful discussions.

## References

- [1] Lackner KS, Butt DP, Wendt CH. Progress on binding CO<sub>2</sub> in mineral substrates. *Energy Convers Manage* 1997;38:S259–64.
- [2] Lackner KS, Wendt CH, Butt DP, Joyce EL, Sharp DH. Carbon dioxide disposal in carbonate minerals. *Energy* 1995;20(11):1153–70.
- [3] Seifritz W. CO<sub>2</sub> disposal by means of silicates. *Nature* 1990;345:486.
- [4] Wicks FJ, O'Hanley DS. In: *Reviews in mineralogy serpentine minerals: structures and petrology*, vol 19. Washington, DC: Mineral Society of America; 1988.
- [5] McKelvy M, Sharma R, Chizmeshya A, Carpenter R, Streib K. Magnesium hydroxide dehydroxylation: In situ nanoscale observations of lamellar nucleation and growth. *Chem Mater* 2001;13:921–6.

- [6] O'Connor WK, Dahlin DC, Nilsen DN, Rush GE, Walters RP, Turner PC. Carbon dioxide sequestration by direct mineral carbonation: Results from recent studies. In: Proceedings of the First National Conference on Carbon Sequestration, Washington DC, NETL, 2001.
- [7] O'Connor WK, Dahlin DC, Turner PC, Walters RP. Carbon dioxide sequestration by ex-situ mineral carbonation. *Technology* 1999;7S:115–23.
- [8] O'Connor WK, Dahlin DC, Nilsen DN, Rush GE, Walters RP, Turner PC. CO<sub>2</sub> storage in solid form: A study of direct mineral carbonation. In: Proceedings of the 5th International Conference on Greenhouse Gas Technologies, Cairns, Australia, 2000. p. 7.
- [9] Luce RW, Bartlett RW, Parks GA. Dissolution kinetics of magnesium silicates. *Geochim Cosmochim Acta* 1972;36:35–50.
- [10] Lin F, Clemency CV. The dissolution kinetics of brucite, antigorite, talc, and phlogopite at room temperature and pressure. *Am Mineral* 1981;66:801–6.
- [11] Tartaj P, Cerpa A, Garica-Gonzalez MT, Serna CJ. Surface instability of serpentine in aqueous suspensions. *J Colloid Interface Sci* 2000;231:176–81.
- [12] Moulder JF, Stickle WF, Sobol PE, Bomben KD. Handbook of X-ray photoelectron spectroscopy. Eden Prairie, Minnesota: Perkin–Elmer; 1992. and references therein.
- [13] Teng H, Dove PM, De Yoreo JJ. Kinetics of calcite growth: Surface processes and relationships to macroscopic rate laws. *Geochim Cosmochim Acta* 2000;64:2255–66.
- [14] Guthrie GD, Carey JW, Bergfeld D, Byler D, Chipera S, Ziock HJ, et al. Geochemical aspects of the carbonation of magnesium silicates in an aqueous medium. In: Proceedings of the First National Conference on Carbon Sequestration, Washington DC, NETL, 2001.
- [15] Berner RA, Holdren Jr GR. Mechanism of feldspar weathering-II. Observations of feldspars from soils. *Geochim Cosmochim Acta* 1979;43:1173–86.
- [16] Berner RA, Sjöberg EL, Velbel MA, Krom MD. Dissolution of pyroxenes and amphiboles during weathering. *Science* 1980;207:1205–6.
- [17] Holdren Jr GR, Berner RA. Mechanism of feldspar weathering -I. Experimental studies. *Geochim Cosmochim Acta* 1979;36:1067–70.
- [18] Schott J, Berner RA, Sjöberg EL. Mechanism of pyroxene and amphibole weathering-I. Experimental studies of iron-free minerals. *Geochim Cosmochim Acta* 1981;43:1161–71.
- [19] Stumm W, Morgan JJ. Aquatic chemistry. New York: John Wiley and Sons; 1996.
- [20] Schnoor JL. The kinetics of chemical weathering: a comparison of laboratory and field weathering rates. In: Stumm W, editor. Aquatic chemical kinetics. New York: John Wiley and Sons; 1990. p. 476.
- [21] De la Caillerie JBD, Kermarec M, Clause O. Si NMR Observation of an amorphous magnesium silicate formed during impregnation of silica with Mg(II) in aqueous solution. *J Phys Chem* 1995;99:17273–81.